

Approach to prevent locking in a spring-damper system by adaptive load redistribution with auxiliary kinematic guidance elements

Christopher M. Gehb^{*a}, Roland Platz^b and Tobias Melz^a

^aSystem Reliability and Machine Acoustics SzM, Technische Universität Darmstadt, Magdalenenstrasse 4, D - 64289 Darmstadt, Germany;

^bFraunhofer Institute for Structural Durability and System Reliability LBF, Bartningstrasse 47, D - 64289 Darmstadt, Germany

ABSTRACT

In many applications, kinematic structures are used to enable and disable degrees of freedom. The relative movement between a wheel and the body of a car or a landing gear and an aircraft fuselage are examples for a defined movement. In most cases, a spring-damper system determines the kinetic properties of the movement. However, unexpected high load peaks may lead to maximum displacements and maybe to locking. Thus, a hard clash between two rigid components may occur, causing acceleration peaks. This may have harmful effects for the whole system. For example a hard landing of an aircraft can result in locking the landing gear and thus damage the entire aircraft. In this paper, the potential of adaptive auxiliary kinematic guidance elements in a spring-damper system to prevent locking is investigated numerically. The aim is to provide additional forces in the auxiliary kinematic guidance elements in case of overloading the spring-damper system and thus to absorb some of the impact energy. To estimate the potential of the load redistribution in the spring-damper system, a numerical model of a two-mass oscillator is used, similar to a quarter-car-model. In numerical calculations, the reduction of the acceleration peaks of the masses with the adaptive approach is compared to the acceleration peaks without the approach, or, respectively, when locking is not prevented. In addition, the required force of the adaptive auxiliary kinematic guidance elements is calculated as a function of the masses of the system and the drop height, or, respectively, the impact energy.

Keywords: adaptive System, kinematic elements, load redistribution, Structural Health Control SHC

1. INTRODUCTION

Defined kinematics are often an important part of the functional performance in load-bearing systems with moving structural components. Examples are landing gear or suspension strut movements in airplanes or vehicles. These movements are provided by kinematic elements, as an auxiliary structure (guest), that link two or more parts of a primer load structure (host) mechanically. The kinematic elements may block degrees of freedom of the various parts of a system so that only a specifically desired movement is possible. In a landing gear, a primer load structure (host) is represented by a piston rod and a cylinder. Torque links are used as an auxiliary kinematic structure (guest) without load-bearing properties in axial direction. In cases of overloading the host, it might be useful to redistribute a part of the load to the guest e.g. with guidance elements capable to bear additional axial loading. Another example is the vertical movement of a car's suspension. In this case a spring-damper system as the host determines the kinetic properties. End-stops as guest restrict the travel range. The limitation of travel range may lead to locking, which occurs e.g. if unexpected and critical high load peaks are applied to a system. High acceleration peaks in car⁻¹ or seat-suspension² or worsening performance in active mass driver (AMD)³ may be a result of exceeding the travel range.

To enhance the dynamic of the system for vibration control today, semi-active systems are used in car- or seat-suspensions, mostly controlled by the sky-hook control strategy.⁴ They can be used to enhance the vertical damping property. They are an opportunity to beat the trade-off between comfort and driving handling for car

* E-mail: gehb@szm.tu-darmstadt.de, Telephone: +49 (0)6151 705 8304

design, but mostly do not take into account problems that may occur when the suspension travel reaches the limit.¹

In this paper, the potential of an active auxiliary kinematic guidance elements (guest) in a spring-damper system (host) with an additional kinetic, load-bearing function to prevent end-stop impact events caused by a drop test is investigated numerically. The aim is to provide additional forces in the auxiliary kinematic guidance elements that absorb kinetic energy in an alternative load path in case of overloading the spring-damper system, e. g. due to exceeding the travel range when hitting the ground after falling from the maximum drop height. The basic idea is to redirect axial loads through the originally kinematic and now kinetic guidance elements, that are normally going through the spring-damper system only. To estimate the potential of the load redistribution, a numerical model of a two-mass oscillator (host) with auxiliary kinematic guidance elements (guest), able to actively bear axial loads, is used. It is derived from a more complex load-bearing system that is currently developed in the German Collaborative Research Center (SFB) 805 “Control of Uncertainties in Load-Carrying Structures in Mechanical Engineering” at the Technische Universität Darmstadt. The acceleration peaks of the upper mass, resulting from the lower mass hitting the ground after simulated drop tests, are compared for with and without the augmented kinetic function of the guidance elements. Furthermore, the relative displacement of the two masses is investigated according to the two cases with and without kinetic function. Eventually, a kinematic transmission variation of the guidance elements due to the kinematic state is shown.

2. MATHEMATICAL DYNAMIC MODEL OF THE TWO-MASS OSCILLATOR

A two-mass oscillator with two degrees of freedom, similar to a quarter-car-model, is used as an example for a dynamic load-bearing system to investigate the ability to redirect parts of the axial load path from the spring-damper system to the additional kinematic guidance elements with an active load bearing capacity, Fig. 1. The

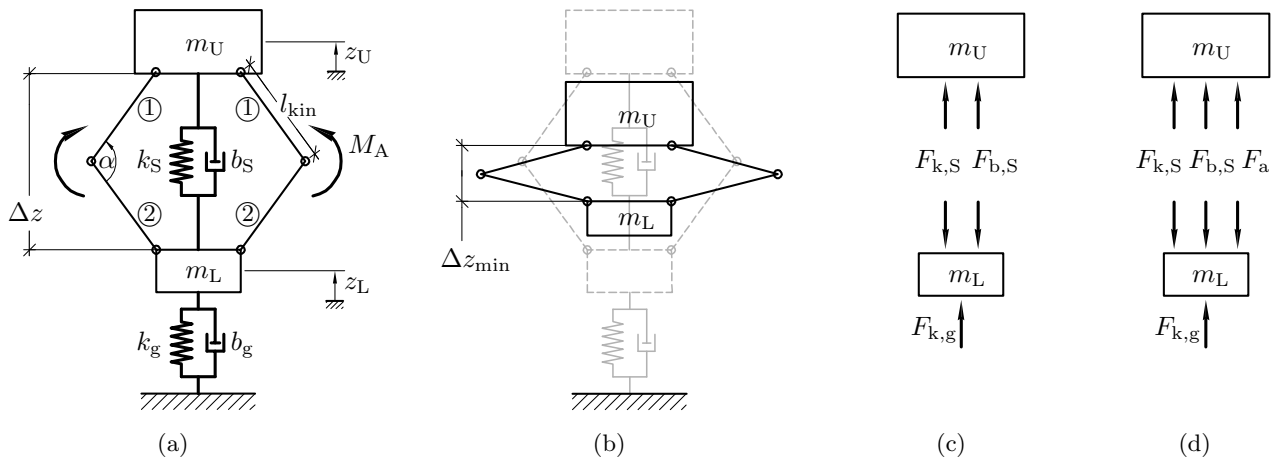


Figure 1. Two-mass oscillator with kinematic guidance elements at $\Delta z = \Delta z_0 := 0$ (a) and at minimal relative displacement Δz_{\min} (b), cut free forces for the passive system without (c) and cut free forces for the active system with additional kinetic function of the guidance elements (d)

two-mass oscillator has an upper and a lower mass m_U and m_L connected by a suspension strut with a coil spring and a viscous damper, with stiffness k_S and damping coefficient b_S . The lower mass m_L is connected to the ground by, again, a spring and a damper with stiffness k_g and damping coefficient b_g . The upper and lower masses are kinematically connected by angular guidance elements with the ability to actively redistribute the load path. The suspension strut and the angular guidance elements are assumed to be free of mass. The cut free spring force and damping force of the suspension strut are

$$F_{k,S} = k_S \Delta z \quad \text{with the relative motion} \quad \Delta z = z_L - z_U, \quad (1a)$$

$$F_{b,S} = b_S \Delta \dot{z} \quad \text{with the relative velocity} \quad \Delta \dot{z} = \dot{z}_L - \dot{z}_U \quad (1b)$$

and the cut free spring force and damping force of the ground are

$$F_{k,g} = k_S z_L, \quad (2a)$$

$$F_{b,g} = 0 \quad (2b)$$

with neglected damping $b_g = 0$ between lower mass and the ground as assumption by the authors. The initial state of the two-mass oscillator at $\Delta z = \Delta z_0 := 0$ is shown in Fig. 1(a), the minimum relative displacement Δz_{\min} of the two masses, limited by assumed end-stops, is shown in Fig. 1(b). The stiffness properties k_S of the strut for motions before and after reaching the end stops is simulated by two different stiffnesses,

$$k_S = \begin{cases} k_{S,1} & \text{for } \Delta z \geq \Delta z_{\min}, \\ k_{S,2} & \text{for } \Delta z < \Delta z_{\min}. \end{cases} \quad (3)$$

with $k_{S,2} = 100 \cdot k_{S,1}$. This means that once the end stop comes into effect, further movement $\Delta z < \Delta z_{\min}$ is still possible, since the end stops are assumed not to be rigid, but with a much higher stiffness $k_{S,2}$ than $k_{S,1}$. When considering a passive system without redirection of load path, the guidance elements have no kinetic use and any additional forces and moments are neglected, Fig. 1(c). When considering an active system with redirection of load path, the guidance elements are able to provide additional moments M_a , Fig. 1(a). The two active moments M_a result in a vertical active force F_a , Fig. 1(d), and are coupled by the kinematic transmission

$$2 \cdot M_a = \cos(\alpha) l_{\text{kin}} F_a, \quad (4)$$

where l_{kin} represents the length of one component ① and ② of the kinematic guidance elements and α the angle between the components ① and ② of the kinematic guidance elements on each side, see Fig. 1(a). The active force

$$F_a = b_a \Delta \dot{z} + k_a \Delta z \operatorname{sgn}(\Delta \dot{z}) \quad (5)$$

is simulated as an assumed control feedback loop with two linear gain factors b_a and k_a for active control. Equation (5) represents a damping force with $b_a \Delta \dot{z}$ proportional to the relative velocity $\Delta \dot{z}$ and $k_a \Delta z \operatorname{sgn}(\Delta \dot{z})$ proportional to the relative displacement Δz in z -direction. Both terms in (5) are dependent on the sign of the relative velocity $\Delta \dot{z}$. The sign function in (5) leads to a case analysis for the gain k_a depending on the relative velocity

$$k_a = \begin{cases} +k_a & \text{for } \Delta \dot{z} > 0, \\ -k_a & \text{for } \Delta \dot{z} < 0. \end{cases} \quad (6)$$

With Eqs. (1a), (1b), (1a), (1b) and (5) according to the displacements z_U and z_L of upper and lower masses m_U and m_L , the two coupled linear equations of motion⁵ for the two degrees of freedom of the masses can be written as

$$m_U \ddot{z}_U + b_S (\dot{z}_L - \dot{z}_U) + k_S (z_L - z_U) = -m_U g + F_a \quad (7)$$

for the upper mass and

$$m_L \ddot{z}_L + b_S (\dot{z}_U - \dot{z}_L) + k_S (z_U - z_L) + k_W z_U = -m_L g - F_a \quad (8)$$

for the lower mass, combined to a linear matrix formulation

$$\underbrace{\begin{pmatrix} m_U & 0 \\ 0 & m_L \end{pmatrix}}_{\mathbf{M}} \underbrace{\begin{pmatrix} \ddot{z}_U \\ \ddot{z}_L \end{pmatrix}}_{\ddot{\mathbf{z}}} + \underbrace{\begin{pmatrix} b_S + b_a & -(b_S + b_a) \\ -(b_S + b_a) & b_S + b_a \end{pmatrix}}_{\mathbf{B}} \underbrace{\begin{pmatrix} \dot{z}_U \\ \dot{z}_L \end{pmatrix}}_{\dot{\mathbf{z}}} + \underbrace{\begin{pmatrix} k_S + k_a & -(k_S + k_a) \\ -(k_S + k_a) & k_S + k_a + k_W \end{pmatrix}}_{\mathbf{K}} \underbrace{\begin{pmatrix} z_U \\ z_L \end{pmatrix}}_{\mathbf{z}} = \underbrace{\begin{pmatrix} -m_U g \\ -m_L g \end{pmatrix}}_{\mathbf{F}}. \quad (9)$$

In Eq. (9), \mathbf{M} , \mathbf{B} and \mathbf{K} are the mass, damping and stiffness matrices, $\ddot{\mathbf{z}}$, $\dot{\mathbf{z}}$, \mathbf{z} and \mathbf{F} are the acceleration, velocity, displacement and force vectors. The force vector \mathbf{F} in (9) contains only the weight forces of the masses m_U and m_L and the gravity g which leads to a static relative displacement Δz_{stat} . The active force F_a in (5) and the considered end-stop stiffness assumption in (3) lead to an overall nonlinear two-mass oscillator in (9). Although, it is possible to get piecewise linear behavior by separating the solution in various sections depending

on the cases in Eq. (3) and Eq. (6) for k_S and k_a . For each section, the homogeneous part of the differential Eq. (9) can be solved with the exponential approach

$$\mathbf{z}(t) = \hat{\mathbf{z}} e^{\lambda t} \quad (10)$$

which leads to the eigenvalue problem

$$[\lambda^2 \mathbf{M} + \lambda \mathbf{B} + \mathbf{K}] \hat{\mathbf{z}} e^{\lambda t} = 0, \quad (11)$$

for the homogeneous form of (9) with the characteristic polynomial

$$P(\lambda) = \det \{ \lambda^2 \mathbf{M} + \lambda \mathbf{B} + \mathbf{K} \}. \quad (12)$$

The solutions of the characteristic polynomial (12) are N pairs of complex conjugate eigenvalues λ_n and λ_n^* for $n=1, \dots, N$. The number of degrees of freedom in case of the two-mass oscillator is $N = 2$. With Eq. (11) the corresponding N pairs of complex conjugate eigenvectors are $\hat{\mathbf{z}}_n$ and $\hat{\mathbf{z}}_n^*$. The free motion of the homogeneous system is the sum of the N modal eigen-oscillations

$$\mathbf{z}_h(t) = \sum_{n=1}^N \hat{\mathbf{z}}_n C_{1n} e^{\lambda_n t} + \hat{\mathbf{z}}_n^* C_{2n} e^{\lambda_n^* t}. \quad (13)$$

The particular part of (9) is taken into account by

$$\mathbf{z}_p = \mathbf{K}^{-1} \mathbf{F} \quad (14)$$

which can be interpreted as a static relative displacement Δz_{stat} due to the weight forces of the masses m_U and m_L . The overall solution is the superposition of (13) and (14) and can be stated as

$$\mathbf{z}(t) = \mathbf{z}_h(t) + \mathbf{z}_p. \quad (15)$$

To calculate the integration constants C_{1n} and C_{2n} in (13), initial conditions presented in the next section are used.

3. NUMERICAL SIMULATION OF DROP TESTS

The numerical solution (15) of the governing Eq. (9) is basis for the following numerical simulations to study the potential of the proposed method for load path redistribution. In Table 1, the assumed values for the introduced variables in (9) are summarized.

In order to solve the solution of (15), initial conditions are used. For that, a drop test with initial velocities for both masses m_U and m_L unequal to zero $\dot{z}_{U,0} = \dot{z}_{L,0} \neq 0$ is taken into account. The initial velocities are calculated by the shift of the potential energy E_{pot} of an assumed drop height h into kinetic energy E_{kin} when falling from that height. This assumption results in the initial velocities $\dot{z}_{U,0} = \dot{z}_{L,0} = \sqrt{2gh}$ for m_U and m_L . By exceeding a maximal drop height h_{max} the system hits the end-stops when the system is falling from h_{max} and hitting the ground. Three different drop test cases are investigated:

- i) drop height $h = h_{\text{max}} = 0.2 \text{ m} \hat{=} \text{max. drop height}$ & passive system without auxiliary kinetic function of the guidance elements,
- ii) drop height $h = 1.2 \cdot h_{\text{max}} = 0.24 \text{ m} \hat{=} 20\% \text{ surplus of max. drop height}$ & passive system without auxiliary kinetic function of the guidance elements,
- iii) drop height $h = 1.2 \cdot h_{\text{max}} = 0.24 \text{ m} \hat{=} 20\% \text{ surplus of max. drop height}$ & active system with auxiliary kinetic function of the guidance elements.

In case iii), the gain factors for F_a according to Eq. (5) are assumed $b_a = 0.2 \cdot b_S$ and $k_a = 0.2 \cdot k_S$. With a defined relation between the gain factors b_a and k_a and the suspension parameters b_S and k_S , it is possible to describe the split of the load path for the active system. The originally kinematic and now kinetic guidance elements become part of the flux of forces and can prevent locking of the system.

Table 1. Parameters of the two-mass oscillator

Property	Variable	Value	Unit
damping (suspension)	b_S	1500	Ns/m
stiffness 1 (suspension)	$k_{S,1}$	27000	N/m
stiffness 2 (suspension)	$k_{S,2}$	2700000	N/m
min. displacement (suspension)	Δz_{\min}	-0.2	m
upper mass	m_U	220	kg
lower mass	m_L	40	kg
damping (ground)	b_g	0	Ns/m
stiffness (ground)	k_g	225000	N/m
gravity	g	9.81	m/s ²

3.1 Decay of acceleration due to cases i-iii)

The two-mass oscillator hits the ground after it is falling down from different drop heights with respect to cases i) to iii). The acceleration decay \ddot{z}_U in time domain according to the three cases i) to iii) after hitting the ground is shown in Fig. 2. The three curves, one for each case i), ii), and iii), start at $t = 0$ s with $\ddot{z}_U = -g = -9.81$ m/s² as a result of the initial conditions for (13). Figure 2 shows $\ddot{z}_U = 0$ m/s² at the end of the decay at $t = 1.5$ s.

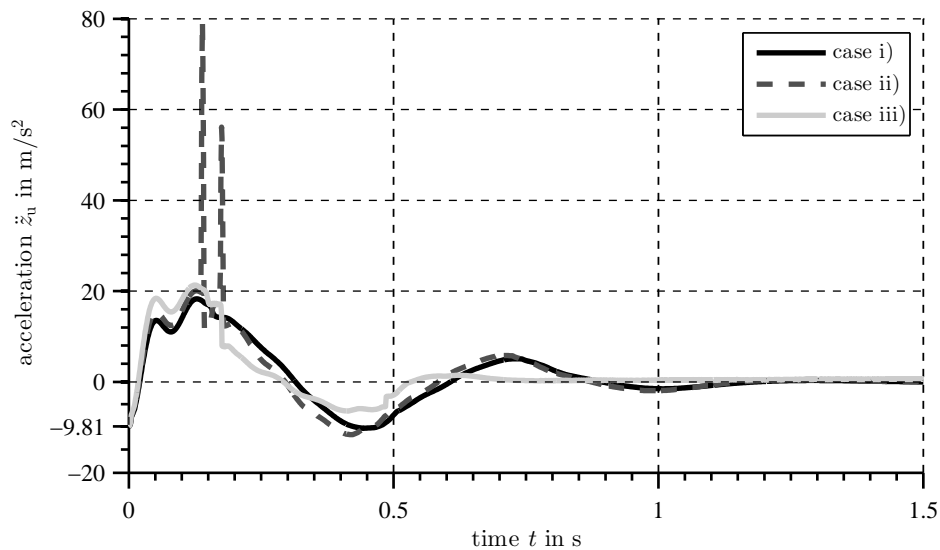


Figure 2. Acceleration \ddot{z}_U of the upper mass m_U for the three cases i-iii)

Case i): After a rebound at the beginning at $t = 0.1$ s influenced by the interaction of the two masses m_L and m_U , the vibrations damp out. The end-stop is not reached.

Case ii): After a short rebound at $t = 0.1$ s similar to case i), the vibrations are not damped out immediately, but two acceleration peaks for \ddot{z}_U can be seen due to the end-stop coming into action. The impact energy of the system due to the drop exceeded the amount of energy the passive system can deal with and the high stiffness $k_{S,2}$ of the end-stop causes the acceleration peaks. After the two end-stop come to effect once, the vibrations damp out.

Case iii): The decay starts again with a short rebound at $t = 0.1$ s influenced by the interaction of the two masses m_L and m_U , similar to cases i) and ii), but with up to 40% higher values for the acceleration caused by the additional force F_a provided in the active guidance elements. Although the values for the acceleration are up to 40% higher than in cases i) and ii) between $t = 0$ s and $t = 0.15$ s, the additional load path through the active kinematic guidance elements prevents the high acceleration peaks and no end-stop effects occur.

3.2 Decay of the relative displacement of the two masses due to cases i-iii)

The two-mass oscillator hits the ground after it is falling down from different drop heights with respect to cases i) to iii). The decay in time domain for the relative displacement Δz of the two masses m_U and m_L according to the three cases i) to iii) after hitting the ground is shown in Fig. 3. The three curves, one for each case i), ii), and iii), start at $t = 0$ s with $\Delta z = \Delta z_0 = 0$ m for the unloaded system and end with a static relative displacement $\Delta z = \Delta z_{stat}$ caused by the weight of the mass m_U at the end of the decay at $t = 1.5$ s. The relative displacement is assumed to be limited by end-stops. The displacement limit is reached at the minimal relative suspension displacement $\Delta z = \Delta z_{min} = -0.2$ m, as presented in Table 1. By exceeding the displacement limit, the suspension strut stiffness $k_S = k_{S,2}$ is high according to (3) and, thus, end-stop comes into effect.

Case i): The relative displacement of the two masses m_U and m_L remains above the minimal displacement, $\Delta z > \Delta z_{min}$, for the whole decay progress. The end-stops are not effective.

Case ii): The relative displacement of the two masses m_U and m_L undercuts the minimal suspension displacement, $\Delta z < \Delta z_{min}$, twice during the decay. The zoom window in Fig. 3 shows the critical area during the decay when the end-stops are reached. The suspension strut stiffness k_S changes from $k_{S,1}$ to $k_{S,2}$ according to (3) and, thus, acceleration peaks in Fig. 2 are observed.

Case iii): The relative displacement of the two masses m_U and m_L remains again above the minimal displacement, $\Delta z > \Delta z_{min}$, for the whole decay. The end-stops are not reached in contrary to case ii). The extremum of the relative displacement is even 7% less compared to case i). The additional force F_a provided by the active guidance elements prevents locking due to an alternative load path.

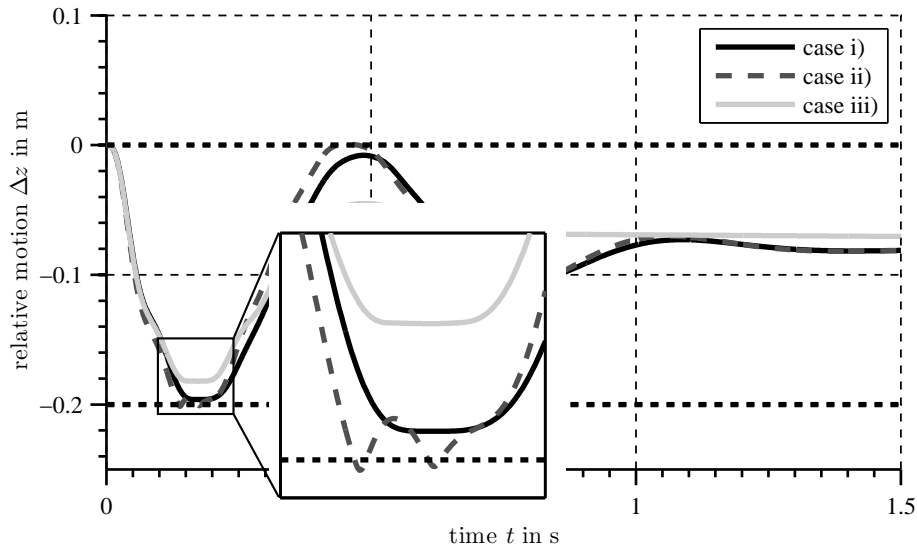


Figure 3. Relative displacement Δz of the upper and lower masses m_U and m_L for the three cases i-iii)

3.3 Resulting Forces at suspension strut and guidance elements

The two-mass oscillator hits the ground after it is falling down from different drop heights with respect to cases i) to iii). The resulting axial forces F_z , $F_{z,S}$ and $F_{z,a}$ of the suspension strut, the suspension strut with additional kinetic function of the active guidance elements and the active elements itself for cases i-iii) according to (1a),

(1b) and (5) during the decay are shown in Fig. 4. All the curves, one for each case i) and ii) and three for iii), begin at $t = 0$ s with $F_z = 0$ N for the unloaded system and end with a static force countering the weight force of the mass m_U at the end of the decay at $t = 1.5$ s.

Case i): The whole load path from the lower mass m_L to the upper mass m_U is led through the suspension strut. The resulting axial force in z -direction is $F_z = F_{k,S} + F_{b,S}$. Since the end-stop is not reached for case i), the stiffness of the suspensions strut according to (3) is $k_S \equiv k_{S,1}$ during the whole decay.

Case ii): The whole load path from the lower mass m_L to the upper mass m_U is led through the suspension strut similar to case i). The resulting axial force in z -direction is again $F_z = F_{k,S} + F_{b,S}$. Since the maximal drop height of the passive system is exceeded, the end-stop is reached twice. The suspension strut stiffness k_S changes from $k_{S,1}$ to $k_{S,2}$ according to (3) when reaching the end-stop and, thus, force peaks with $F_{z,ii} \gg F_{z,i}$ can be observed in Fig. 4.

Case iii): The load path from the lower mass m_L to the upper mass m_U is split into a part in the suspension strut $F_{z,S} = F_{k,S} + F_{b,S}$ and a part in the active kinetic guidance elements $F_{z,a} = F_a$, dashed light gray curves. The resulting axial force in z -direction is the sum of the suspension strut force and the additional force $F_z = F_{z,S} + F_{z,a}$, solid light gray curve. Although the maximal drop height of the passive system is exceeded, the end-stop is not reached by means of the active kinetic guidance elements. The stiffness of the suspension strut according to (3) is $k_S \equiv k_{S,1}$ during the whole decay comparable to case i). Since the additional force F_a according to (5) depends on the algebraic sign of the relative velocity $\Delta\dot{z}$, the force F_a changes its algebraic sign in the same manner as the relative velocity $\Delta\dot{z}$ does. This can be seen in the zoom window in Fig. 4.

Considering Figures 2-4, it can be seen that active kinetic guidance elements has potential to provide an alternative load path in a load-bearing system. Depending on the assumed control law in (5), the distribution of the load between the suspension strut and the guidance elements can be adjusted.

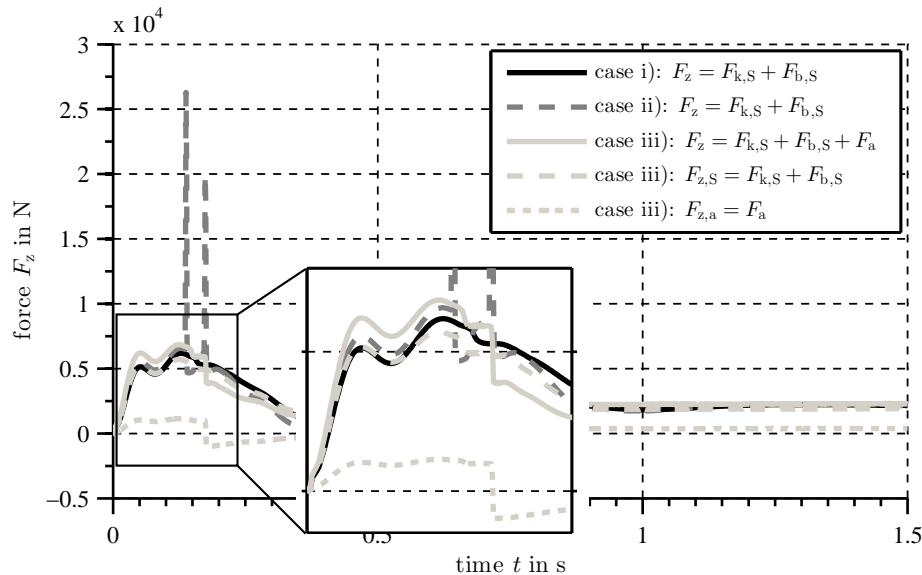


Figure 4. Resulting axial forces F_z and $F_{z,S}$ at the suspension strut and active force $F_{z,a} = F_a$ for the three cases i-iii)

3.4 Influence of the kinematic transmission of the guidance elements

Figure 5 shows the kinematic transmission due to varying angles α and their influence of the required moments M_a to maintain sufficient active forces F_a for load path redistribution. In this Paper, the active axial force F_a is provided by active kinetic guidance elements due to two active moments M_a according to (4) and Fig. 1. Because of the kinematic transmission of the guidance elements, a constant axial force F_a requires an increasing active moment M_a for decreasing angle α , cf. Fig. 1(a) and 1(b). A decreasing angle α is equivalent to a decreasing

relative displacement Δz of the upper and the lower masses m_U and m_L . The range of the angle $\alpha = 130^\circ \dots 50^\circ$ is limited by the assumed end stops at Δz_{\min} . A transmission factor for the required active moments $M_a(\alpha)$ for a constant active axial force F_a depend on the angle α and can be stated as

$$\gamma = \frac{M_a(\alpha)}{M_a(130^\circ)} \quad (16)$$

with the minimal required active moment $M_a(130^\circ)$ at the widest possible angle $\alpha = 130^\circ$ as reference on one side in Fig. 1(a). The transmission factor γ is shown in Fig. 5. At $\alpha = 130^\circ$ the transmission factor is $\gamma = 1$. For $\alpha < 65^\circ$, the transmission factor is $\gamma \geq 2$ and, thus, the required active moment M_a for a constant vertical force F_a has doubled.

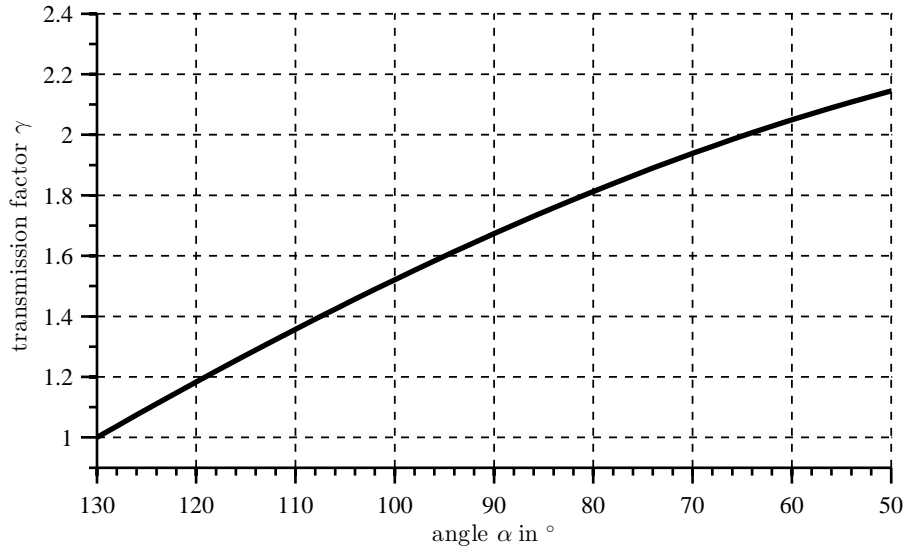


Figure 5. kinematic transmission γ factor of the angular guidance elements

4. CONCLUSION

This paper shows the potential of an active auxiliary kinetic guidance elements in a two mass spring-damper system to prevent end-stop impact events by changing the load path after the system hits the ground according to different drop heights. By changing the load path, load redistribution leads to less loading of the otherwise high loaded suspension strut alone. The system is simplified by a two-mass oscillator with two degrees of freedom. Three cases i-iii) are taken into account: case i) a drop test from maximal drop height for the passive system without auxiliary kinetic function of the guidance elements, case ii) a drop test from 20 % exceeded maximal drop height for the passive system without auxiliary kinetic function of the guidance elements and case iii) a drop test from 20 % exceeded maximal drop height for the active system with auxiliary kinetic function of the guidance elements. For all cases i-iii), the acceleration of the upper mass, the relative displacement and the resulting axial forces between the masses are calculated. Case i) is used as reference without end-stop effects and only one load path that goes through the suspension strut. Case ii) leads to undesirable high relative displacements of the two masses and, thus, to end-stop effects causing high acceleration peaks. As in case i), only one load path that goes through the suspension strut is available in case ii). In case iii), the load path is split into a part in the suspension strut and a part in the active kinetic guidance elements. Despite exceeded drop height, dangerous end-stop effects that lead to high impacts, are prevented. It is shown that a kinematic transmission of the angular guidance elements increases the required moments M_a to maintain sufficient active forces F_a for load path redistribution. Although, active kinetic guidance elements can be used to prevent locking in case of overloading or to provide fail-safe behavior in case of a damaged primary load path due to redirecting the load partly through an alternative load path.

ACKNOWLEDGMENTS

The authors like to thank the German Research Foundation (DFG) for funding this project within the Collaborative Research Center (SFB) 805 “Control of Uncertainties in Load-Carrying Structures in Mechanical Engineering”.

REFERENCES

- [1] Do, A. L., Spelta, C., Savaresi, S., and Sename, O., “An lqv control approach for comfort and suspension travel improvements of semi-active suspension systems,” *IEEE Conference on Decision and Control* **49**, 5560–5565 (2010).
- [2] Wu, X. and Griffin, M. J., “A semi-active control policy to reduce the occurrence and severity of end-stop impacts in a suspension seat with an electrorheological fluid damper,” *Journal of Sound and Vibration* **203**, 781–793 (1997).
- [3] Venanzi, I., Ubertini, F., Ierimonti, L., and Materazzi, A. L., “Non-linear control strategy for handling stroke limits of an active mass driver system,” *Proc. 6th WCSCM*, 931–945 (2014).
- [4] Unger, A. F., *Serietaugliche quadratisch optimale Regelung für semiaktive Pkw-Fahrwerke (engl. Series-ready quadratic optimal control for semi-active passenger car chassis)*, PhD thesis, Technische Universität München (2012).
- [5] Markert, R., [*Strukturdynamik (engl. Structural Dynamics)*], Shaker Verlag (2013).